

## Intelligent interpretation of digital images of rock joints based on pattern recognition

FAN Liuming<sup>1,2\*\*</sup> and LI Ning<sup>1</sup>

(1. Xi'an University of Technology, Xi'an 710048, China; 2. Chang'an University, Xi'an 710054, China)

Received August 22, 2003; revised September 23, 2003

**Abstract** As a composition of rockmass, structural planes are one of the chief factors that can largely control the mechanical response of rockmass and its models of deformation and failure under the action of engineering load. Rock joints are a typical sort of structural planes, which are numerous, random and universal in the rockmass. So the measurement and statistics of rock joints are the basics for classifying rockmass grades, evaluating rockmass quality, and selecting physico-mechanical parameters of rockmass. However, the traditional *in situ* investigation using manual measuring tools is inefficient and costly. In order to improve the above-mentioned status, new methods to measure joints should be developed, which should be efficient, simple and convenient. The rapid developments of modern digital photography and digital image processing make it possible that digital photograph devices such as digital cameras or digital videos can be used to measure joints. So based on theories and methods of pattern recognition and image processing, the intelligent interpretation of digital images of rock joints is studied, and the corresponding computational method is also put forward for the first time. The procedure and results of intelligent interpretation of a joint image have been discussed in detail.

**Keywords:** rock joints, pattern recognition, digital images of rock joints, intelligent interpretation.

Separated by structural planes, natural rocks are broken up into the rock block system, which has the characteristics of discontinuity, anisotropism and inhomogeneity. The concept of rockmass structure and the viewpoint that the rockmass stability is controlled by its structure were put forward by Gu and Sun<sup>[1,2]</sup> in the 1960s. In the 1980s, the controlling theory of rockmass structure was brought forward by Sun, and the basic regularities of deformation and failure of rockmass were also discussed in detail<sup>[3]</sup>. Because structural planes play a vital role in controlling the mechanical response and the stability of engineering rockmass, much research has been concentrated on properties of rockmass structure<sup>[4]</sup>, especially in the large-scale hydrodynamic engineering. Of all the properties of rockmass structure, geometrical properties of structural planes are still the essentials. International Society for Rock Mechanics (ISRM) in 1978 suggested ten indexes for describing their geometrical properties, such as orientation, spacing, persistence, aperture, roughness, seepage, compressive strength, etc.<sup>[5]</sup>. However, all of them can only be obtained from field surveys.

Joints are a typical sort of structural planes in the rockmass. Owing to their large quantities and universal distribution at random, joints should be investigat-

ed, measured and statistically calculated for classifying rockmass grades, evaluating rockmass quality, and selecting physico-mechanical parameters of rockmass. However, by using either scanline surveys<sup>[6,7]</sup> or scanarea surveys<sup>[8,9]</sup>, the traditional field surveys of geological structural planes are still being on the level of manual operation. With the simple and crude manual tools, such as hammers, magnifiers, and various rulers, field surveys are inefficient, costly and laborious. Therefore, it is an earnest desire to many geotechnical engineers and technicians that the traditional measurement has to be replaced by the new methods based on state-of-the-art techniques. Fortunately, with the rapid development of modern digital photography and digital image processing, some digital photograph devices, such as digital cameras or digital videos, can be used to measure joints. A set of rock joints were photographed with digital videos by Wu<sup>[10]</sup>, who used the AutoCAD software, and based on the optical imaging theory, to study the geometrical relationship between image joints and real joints. Although identifying rock joints still requires manual operation, this is the first attempt to improve the efficiency of structural planes measurement. In order to automatically identify the rock joints by computers, and based on pattern recognition and image processing, we present an intelligent interpretation method

\*\* To whom correspondence should be addressed. E-mail: fanliuming@hotmail.com

of rockmass digital images in this paper.

### 1 The intelligent recognition of image joints

Pattern recognition is also called image recognition, which is defined to classify and recognize digital images according to their features<sup>[11]</sup>. In other words, pattern recognition is to mark off several pixel sets, each with similar pixels, according to some typical features of these digital images. Based on this, what pixel sets stand for is recognized. The purpose of pattern recognition is that some recognition originally done by hand is replaced by intelligent machines<sup>[12]</sup>. Generally speaking, patterns recognition includes three steps<sup>[13]</sup>: image segmentation, feature extraction and classification.

#### 1.1 Image segmentation

Image segmentation<sup>[14]</sup> is to divide a digital image into several nonoverlapping segments, which can separate the recognizing objects from the image backgrounds. As to rock joint images, joints are objects, and others are backgrounds. The purpose of image segmentation is to separate the joints from complicated backgrounds.

There are three sorts of main methods for image segmentation, called region method, boundary method and edge method. In our study, the region method is used. In order to enhance joint images, the edge detection has been done before image segmentation.

**1.1.1 Edge detection** Edge detection is done by differential algorithms, such as gradient (one order differential) algorithm, Laplace (two order differential) algorithm and template matching algorithm. As one of the differential algorithms, template matching algorithm has the superiority to smoothing noise. There are several types of templates for edge detection, such as Robison template<sup>[15]</sup>, Sobel template<sup>[16]</sup>, Prewitt template<sup>[17]</sup>, Kirsh template<sup>[18]</sup>, and Gauss-Laplace template<sup>[19]</sup>.

In fact, the template matching method is one of anisotropic edge detection. Each type of template may include several orient templates, each of which is a  $N \times N$  matrix. As shown in Fig. 1, Robison template includes eight orient templates named  $m_1, m_2, \dots, m_8$ , respectively, and each of them is a  $3 \times 3$  matrix. The matching orientation of each template is consistent with its corresponding arrowhead. The

edge detection based on Robison template can be calculated from the following equation:

$$f_{i,j} = \max_{1 \leq p \leq 8} \sum_{k=1}^3 \sum_{l=1}^3 g_{i+k-2, j+l-2} c_{k,l}(m_p), \quad (1)$$

where  $g$  is the image data;  $i$  and  $j$  are the horizontal coordinate and vertical coordinate of a pixel, respectively;  $c$  and  $p$  are the coefficient and the serial number of the template ( $p = 1, 2, \dots, 8$ ).

**1.1.2 Threshold transform** As one of the region segmentation methods, threshold transform is widely used. The threshold transform function  $f(x, y)$  can be expressed as:

$$f(x, y) = \begin{cases} 1 & g(x, y) \geq \xi, \\ 0 & g(x, y) < \xi, \end{cases} \quad (2)$$

where  $g$  is image data, and  $\xi$  is the threshold. Eq. (2) indicates that the objects are composed of the image pixels, with  $g(x, y)$  values not smaller than  $\xi$ . So the image will be divided into two types of data sets by Eq. (2): one stands for objects, and the other for background. This processing method is also called binarization. Gray images can be converted into black and white ones by binarization.

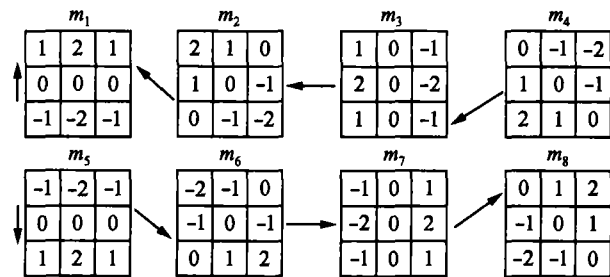


Fig. 1. Robison template<sup>[15]</sup>.

#### 1.2 Feature extraction

Feature extraction should be done after image segmentation. It requires that the features, which can identify a type of objects, are chosen from feature sets. Considering approximate linearity of the joints, the joints can be regarded as straight segments, and be described as polar coordinates  $(\rho, \theta)$ . For the convenience of next process, Hough transform should be performed.

**1.2.1 Hough transform** Any line equation  $y = mx + b$  may be expressed as follows<sup>[20]</sup>:

$$\rho = x \cos(\theta) + y \sin(\theta), \quad (3)$$

where  $\rho$  is the distance from origin to line  $y = mx + b$ , and  $\theta$  is the angle between  $x$ -axis and the line perpendicular to line  $y = mx + b$  (see Fig. 2(a)). Eq. (3) indicates that any line in  $x$ - $y$  plane corresponds

to a unique point in  $\rho$ - $\theta$  plane, and any point in  $x$ - $y$  plane corresponds to a unique sinusoid in  $\rho$ - $\theta$  plane. Apparently, if there are a group of points on the same straight line in  $x$ - $y$  plane (see Fig. 2(b)), the corresponding sinusoids in  $\rho$ - $\theta$  plane must converge at the same point (see Fig. 2(c)).

In order to locate the straight segments in an im-

age,  $\rho$ - $\theta$  plane is discreted into a series of grids, each of which is denoted by  $\rho_j$  and  $\theta_j$ . The discriminant function  $Hf(\rho_j, \theta_j)$  ( $j = 1, \dots, m$ ) is also defined by counting the number of points at the same straight segment corresponding to  $(\rho_j, \theta_j)$  in  $\rho$ - $\theta$  plane. If local extremum of function  $Hf$  exists in a dual coordinate point  $(\rho_j, \theta_j)$ , then the point corresponds to an actual straight segment.

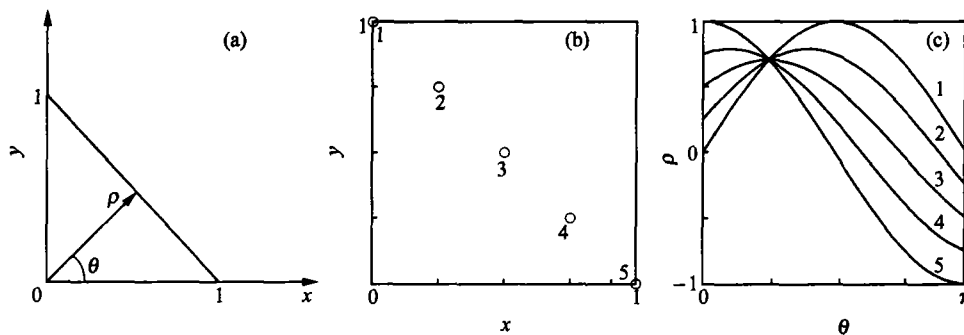


Fig. 2. Hough transform<sup>[13]</sup>. (a) Polar coordinate expression of a line; (b)  $x$ - $y$  plane; (c)  $\rho$ - $\theta$  plane.

**1.2.2 Feature selection** By Hough transform, a line in  $x$ - $y$  plane is processed into a point in  $\rho$ - $\theta$  plane. In other words, any line is described by a point  $(\rho_j, \theta_j)$  uniquely. According to the discriminant function  $Hf(\rho_j, \theta_j)$ , straight segments can be detected. It is reasonable that  $\rho$  and  $\theta$  should be selected to be feature parameters.

**1.3 Classification**

Classification is the last step of pattern recognition of digital images. As to rock joint images, the task of classification is to discriminate between joints and background. In other words, classification is required to decide which point  $(\rho_j, \theta_j)$  in the plane represents a joint, and which does not. As a matter of fact, whether a point in  $\rho$ - $\theta$  plane stands for a real joint depends on whether it makes the discriminant function  $Hf$  locally extreme. Virtually, the discriminant problem for joints is searching for local extremum. Its computational scheme is as follows:

(i) Sort. In terms of the value of  $Hf(\rho_j, \theta_j)$ , data set  $(\rho_j, \theta_j)$  ( $j = 1, \dots, m$ ) is sorted from its maximum to its minimum, i.e.

$$Hf(\rho_1, \theta_1) \geq Hf(\rho_2, \theta_2) \geq \dots \geq Hf(\rho_m, \theta_m). \tag{4}$$

(ii) Search for the first joint. After the threshold  $Hf_\xi$  is selected, the first joint may be found by using the following method:

if  $Hf(\rho_1, \theta_1) > Hf_\xi$ , point  $(\rho_1, \theta_1)$  stands for an actual joint, and it is also the longest one, which is denoted by  $J_1(\rho_0^1, \theta_0^1)$ , and  $\rho_0^1 = \rho_1$ ,  $\theta_0^1 = \theta_1$ . If  $Hf(\rho_1, \theta_1) \leq Hf_\xi$ , then none of the joints are in the image.

(iii) Search for other joints. If  $Hf(\rho_j, \theta_j) \leq Hf_\xi$ , ( $j = 2, \dots, m$ ), classification is finished. If  $Hf(\rho_1, \theta_1) > Hf_\xi$ , then search for next joint. Its algorithm is as follows:

If there are  $k$  joints recognized from the image, which are  $J_1(\rho_0^1, \theta_0^1), J_2(\rho_0^2, \theta_0^2), \dots, J_k(\rho_0^k, \theta_0^k)$ , respectively, the distance  $d_s$  from  $(\rho_j, \theta_j)$  ( $j = k + 1, \dots, m$ ) to respective joints is defined as:

$$d_s = \sqrt{(\rho_j - \rho_0^s)^2 + (\theta_j - \theta_0^s)^2}, \quad (s = 1, \dots, k). \tag{5}$$

According to scale between images and object, the short distance  $d_{\min}$  is decided at first. If  $d_s \leq d_{\min}$ ,  $(\rho_j, \theta_j)$  will belong to joint  $J_s(\rho_0^s, \theta_0^s)$  ( $s = 1, \dots, k$ ). If any  $d_s$  ( $s = 1, \dots, k$ ) is not less than  $d_{\min}$ , then the point  $(\rho_j, \theta_j)$  stands for the  $k + 1$ th joint, which is denoted by  $J_{k+1}(\rho_0^{k+1}, \theta_0^{k+1})$ , and  $\rho_0^{k+1} = \rho_j, \theta_0^{k+1} = \theta_j$ .

(iv) Search for the last joint. Repeat step (iii) until  $Hf(\rho_1, \theta_1) \leq Hf_\xi$ .

## 2 Application of a digital joint image

### 2.1 Trait of the digital joint image

Fig. 3 is one of the digital images of sandstone joints taken by the digital camera Nikon E995 made in Japan. When being photographed, camera lens is kept to be perpendicular to sandstone surface for the sake of geometrical rectification of joint images. The original image of Fig. 3 is true color with 24 bits,  $1024 \times 768$  pixels and JPEG format. In the process of intelligent interpretation, it is converted to 8 bits,  $256 \times 192$  pixels and BMP format. As shown in Fig. 3, there are two joints named  $J_1$  and  $J_2$ , respectively. They are closely parallel to each other, inclination angles of each approach  $45^\circ$  or so. Gray values of two joints are quite less than those of background, so both are darker than background.



Fig. 3. Joint image ( $256 \times 192$ ).

### 2.2 Intelligent interpretation procedure

The corresponding computational program is written according to the above-mentioned procedure. By using this program, intelligent interpretation of Fig. 3 has been done, and the computational results are shown in Fig. 4.

Fig. 4(a) is the result of Robison edge detection from Fig. 3. It can be seen that the joints are white, while the background is dark. It shows that the contrast between the joints and the background has been improved, and effects of image enhancement have been obtained.

Fig. 4(b) is the result of image segmentation from Fig. 4(a). It is a black and white image, in which there are only two kinds of gray values, i. e. 0 (black) or 255 (white). In spite of the occurrence of partial noises in Fig. 4(b), the shapes of two joints can still be obviously distinguished.

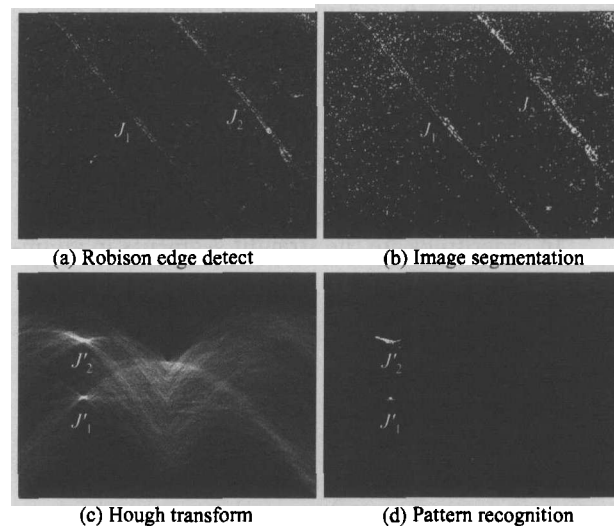


Fig. 4. Intelligent interpretation procedure of joint image.

In order to compute the exact position of joints, Hough transform is done next. In the process of Hough transform, only white pixels are counted. Fig. 4(c) presents the result of Hough transform, where  $\rho$  is an absolute value and varies from 0 to 320 pixels (horizontal direction) as  $\theta$  ranges from  $0^\circ$  to  $180^\circ$  (vertical direction). By Hough transform, linear joints  $J_1$  and  $J_2$  (see Fig. 3) proceed into punctated joints  $J'_1$  and  $J'_2$ . Because joint  $J_1$  is nearly parallel to joint  $J_2$ , the value  $\theta$  of joint  $J_1$  is nearly equal to that of joint  $J_2$ . However, the distance from joint  $J_1$  to the origin (bottom left corner) is shorter than the distance from joint  $J_2$  to the origin, so the value  $\rho$  of joint  $J_1$  is less than that of joint  $J_2$ , showing that the results shown in Fig. 4(c) should be reliable.

Finally, classification is carried out to decide which point  $(\rho_j, \theta_j)$  represents a joint, and which point  $(\rho_j, \theta_j)$  does not. In terms of the above-mentioned procedure, a couple of joints are recognized (see Fig. 4(d)). In most cases, the shape of every joint in  $\rho$ - $\theta$  plane is a small region, not always a point. In order to determine reasonable positions of joints, their region centers are taken as the reference. Based on this, positions of joints are computed, which lie at point  $J'_1(142, 40^\circ)$  and point  $J'_2(224, 37^\circ)$  in  $\rho$ - $\theta$  plane, respectively.

## 3 Conclusion

The measurement based on digital photograph provides us a possible way to improve the measurement efficiency. To investigate its feasibility, the interpretation method for digital images of rock joints is

introduced in this paper. Based on the theory of pattern recognition and image processing, the intelligent interpretation for joint images is put forward, and an application is also given, which has verified that investigation of rock joints based on digital photograph is feasible, and worthy of researching further.

## References

- 1 Gu, D. Z. Foundation of Geological Mechanics for Rockmass Engineering. Beijing: Science Press, 1979, 198~260.
- 2 Sun, Y. K. et al. Study on Engineering Geology for Rocky Slope. Beijing: Geological Science, 1965.
- 3 Sun, G. Z. Mechanics of Rockmass Structure. Beijing: Science Press, 1988, 1~45.
- 4 Zhong, Z. Y. et al. Analytical Theory of Engineering Geology. Beijing: Geology Press, 1994, 6~41.
- 5 ISRM. Suggested methods for the quantitative description of discontinuities in rockmasses. Int. J. Rock Mechanics and Mining Science, 1978, 15(6): 319.
- 6 Priest, S. D. et al. Estimation of discontinuity spacing and trace length using scanline surveys. Int. J. Rock Mech. Min. Sci. Geomech., 1981, 18: 183.
- 7 Sen, Z. et al. Discontinuity spacing and RQD estimates from finite length scanline. Int. J. Rock Mech. Min. Sci. Geomech., 1984, 21(4): 203.
- 8 Laslett, G. M. Censoring and edge effects in areal and line transect sampling of rock joint traces. Mathematical Geology, 1982, 14(2): 125.
- 9 Kulatilake, P. H. S. W. et al. Estimation of mean length of discontinuity. Rock Mech. Rock Eng., 1984, 17: 215.
- 10 Wu, Z. Y. The application of digital image interpretation in the statistics of rock joints in field. Journal of Chengdu University of Technology, 2001, 28(supp): 157.
- 11 Cheng, M. D. et al. Introduction to Image Pattern. Shanghai: Shanghai Technology Press, 1982, 1~8.
- 12 Yang, G. Z. et al. Pattern Recognition. Hefei: Chinese University of Technology Press, 2001, 1~6.
- 13 Castleman, K. R. Digital Image Processing. Beijing: Electronic Industry Press, 2002, 375~394.
- 14 Haralick, R. M. et al. Survey: Image Segmentation. Comput. Vision, Graphics, Image Proc., 1985, 29: 100~132.
- 15 Wang, J. F. et al. Computer Image Recognition. Beijing: Chinese Railway Press, 1988, 82~98.
- 16 Davis, L. S. et al. A survey of edge detection technique. GGIP, 1975, 4: 248.
- 17 Prewitt, J. Object enhancement and extraction. In: Picture Processing and Psychopictorics. New York: Academic Press, 1970.
- 18 Kirsh, R. A. Computer determination of the constituent structure of biological image. Computers in Biomedical Research, 1971, 4: 315.
- 19 Lü, F. J. Introduction to Digital Image Processing. Beijing: Tsinghua University Press, 1999, 136~140.
- 20 Duda, R. E. et al. Pattern Classification and Scene Analysis. New York: Wiley, 1973.